

LA-6754-PR

Progress Report

C.3

**CIC-14 REPORT COLLECTION
REPRODUCTION
COPY**

Special Distribution

Issued: March 1977

**Applied Nuclear Data
Research and Development**

October 1—December 31, 1976

Compiled by

**C. I. Baxman
P. G. Young**



**los alamos
scientific laboratory**

of the University of California

LOS ALAMOS, NEW MEXICO 87545



An Affirmative Action/Equal Opportunity Employer

The four most recent reports in this series, unclassified, are LA-6266-PR, LA-6472-PR, LA-6560-PR, and LA-6723-PR.

This work was performed under the auspices of the Nuclear Regulatory Commission, the Electric Power Research Institute, and the US Energy Research and Development Administration's Divisions of Military Application, Reactor Development and Demonstration, Physical Research, and Magnetic Fusion Energy.

This report was prepared as an account of work sponsored by the United States Government. Neither the United States nor the United States Energy Research and Development Administration, nor any of their employees, nor any of their contractors, subcontractors, or their employees, makes any warranty, express or implied, or assumes any legal liability or responsibility for the accuracy, completeness, or usefulness of any information, apparatus, product, or process disclosed, or represents that its use would not infringe privately owned rights.

CONTENTS

I.	THEORY AND EVALUATION OF NUCLEAR CROSS SECTIONS.....	1
	A. R-Matrix Analysis and Related Activities for Light Systems.....	1
	B. Phenomenological Fit to Experimentally Determined Level Density Parameters.....	2
	C. Nuclear Data for (p,n) Reactions.....	3
	D. Optical Model and Coupled-Channel Analysis.....	4
	E. $n + {}^{237}\text{Np}$ Evaluation	4
	F. Neutron Kermas from ENDF/B Data.....	4
	G. Evaluated Time-Dependent Electron and Photon Spectra Following a Fission Burst.....	6
II.	NUCLEAR CROSS-SECTION PROCESSING.....	7
	A. NJOY Development.....	7
	B. Thermal Power Reactor Cross Sections.....	8
	C. NJOY Photon Processing Validation.....	8
	D. CCCC Interface Files.....	9
	E. NJOY Plotting Module.....	9
	F. Photon Data for Uranium Survey.....	10
	G. Elastic Scattering Matrix for 1DX.....	11
	H. ENDF/B-IV Update.....	12
III.	MAGNETIC FUSION ENERGY -- EPR COVARIANCE DATA LIBRARY....	12
IV.	FISSION-PRODUCT, ACTINIDE, AND DECAY DATA.....	13
	A. Fission-Yield Theory.....	13
	B. ENDF/B Phenomenological Yield Model Improvements.....	14
	C. Fission-Product Data for Thermal Reactors.....	15
	D. Fission-Product Absorption Cross Sections for PWR Applications.....	15
	E. Photoneutron Spectra.....	17
	F. HTGR Burnup Calculations.....	17
	G. ANS 5.1 Decay Heat Standard.....	18
	H. Source Terms for Spent Fuel Accident.....	18
	I. CSEWG Fission Product Yields Subcommittee Meeting....	18
	J. Actinide Chains.....	18
	K. Decay-Heat Beta Spectra.....	18
	REFERENCES.....	20

LOS ALAMOS NATIONAL LABORATORY



3 9338 00396 3948

APPLIED NUCLEAR DATA RESEARCH AND DEVELOPMENT
QUARTERLY PROGRESS REPORT
October 1 - December 31, 1976

Compiled by

C. I. Baxman and P. G. Young

ABSTRACT

This progress report describes the activities of the Los Alamos Nuclear Data Group for the period October 1 through December 31, 1976. The topical content is summarized in the contents.

I. THEORY AND EVALUATION OF NUCLEAR CROSS SECTIONS

A. R-Matrix Analysis and Related Activities for Light Systems (G. Hale)

1. ${}^7\text{Li}$ System. An extension of the ${}^7\text{Li}$ analysis upon which the ENDF/B-V neutron cross sections for ${}^6\text{Li}$ at low energies are based is nearing completion. This analysis includes most of the data available for reactions open below 10.5 MeV excitation energy and provides an interpretation of many features of the data in terms of resonances. Accurate values for the positions and widths of the resonances have been obtained using the RESPAR code described below. These results will be reported in detail at the March Symposium on Neutron Standards and Applications in Washington, D. C.

2. ${}^4\text{He}$ System. Data for the $\text{D}(d,n)$ and $\text{D}(d,p)$ reactions at deuteron energies below 1 MeV have been added to the 2-channel ($p\text{-T}$, $n\text{-}{}^3\text{He}$) analysis described last quarter. While the polarization data for both branches of the $\text{D}+\text{D}$ reaction are adequately represented, the charge-independent fit has difficulty reproducing the larger cross section and 0 to 90° cross-section asymmetry observed for the neutron branch above $E_d = 100$ keV. Although we are able to obtain a slight enhancement of the neutron branch at energies near 1 MeV due to the presence of isospin-one levels, it is not as large as measurements indicate. We are continuing study of this problem.

3. Covariance Matrices for Standard Cross Sections. Using the covariances of the R-matrix parameters from which the standard ${}^6\text{Li}(n,\alpha)$ and ${}^{10}\text{B}(n,\alpha)$ cross sections were calculated for ENDF/B-V, covariance matrices have been constructed for the neutron cross sections of ${}^6\text{Li}$ and ${}^{10}\text{B}$ using standard propagation of error techniques. These covariances will soon be binned and converted to ENDF format for inclusion in the Version V files for ${}^6\text{Li}$ and ${}^{10}\text{B}$ at low energies.

4. Resonance Parameters. An improved code for finding external positions and widths of resonances from R-matrix parameters has been developed in the past quarter. The code (RESPAR), which is based on an earlier program written by R. Nisley (now at Tetra Tech, Arlington, Va.), uses a rapidly converging iteration scheme to search for the poles and residues of the resonant Q matrix, defined in terms of the R-matrix for boundary condition B, the shift S, and penetrability P, by

$$Q_R = P^{1/2} [1 - R(SB)]^{-1} R P^{1/2} .$$

This is a multilevel extension of the prescription commonly used to define resonance parameters in the single-level case.

B. Phenomenological Fit to Experimentally Determined Level Density Parameters (E. D. Arthur)

Level density parameter values play an important role in statistical model calculations such as those made with GNASH. In particular, the value of the observed level spacing, $\langle D \rangle$ (which can be related back to the level density parameter), is extremely important in the calculation of (n,γ) cross sections for neutron energies generally less than a few MeV.

The need to calculate (n,γ) cross sections for nuclei where values of $\langle D \rangle$ do not exist led us to develop a systematic fit to experimentally determined level density parameters. The method chosen was similar to that of Ignatyuk et al.¹ in which the level density parameter a is determined from the shell correction to the mass formula δW . In their fit, Ignatyuk et al.¹ also include a dependence of the level density parameter on excitation energy. Thus, $a(U)$ is given by

$$a(U) = \hat{a} [1 - f(U)\delta W/U] ,$$

where \hat{a} is the asymptotic value of a at high excitation energies, U is the excitation energy (minus pairing effects), and δW is the shell effect parameter described above. The function $f(U)$ was chosen to have the form

$$f(U) = [1 - \exp(-\gamma U)] \quad ,$$

which approximates theoretical forms obtained from calculations of the square of the entropy of a nucleus, $S^2(U)$, using Nilsson and Woods-Saxon potentials.^{2,3}

Experimental values of $\langle D \rangle$ for 200 nuclei were obtained from recent compilations of Baba⁴ and Dilg et al.,⁵ and the values of the level density parameter a were determined using the Gilbert-Cameron level density expression form.⁶ Figure 1 shows the ratio of experimental to calculated value of $\langle D \rangle$ using the parameters of Cook et al.⁷ while Fig. 2 shows the results of the present fit. A factor of 10 improvement in reduced χ^2 was obtained. Also, this excitation-energy-dependent form of a is more realistic in that at high excitation energies, shell effects present at lower energies are reduced. This behavior is more realistic in light of detailed theoretical treatments of the level density behavior in various nuclei.⁸

C. Nuclear Data for (p,n) Reactions (E. D. Arthur)

Cross sections for charged-particle-induced nuclear reactions on medium or heavy-mass nuclei are sometimes used as radioactive monitors for certain nuclear reactions. The preequilibrium-statistical model code GNASH has been utilized to satisfy requests for charged-particle-induced nuclear data. In particular, cross sections for (p,n) reactions leading to radioactive product nuclei have been calculated for the following cases: ^{45}Sc , ^{89}Y , ^{90}Zr , ^{169}Tm , ^{175}Lu , ^{191}Ir , ^{193}Ir , and ^{197}Au .

Calculations such as these involving charged-particle reactions provide an opportunity to test preequilibrium parameters used in the calculation of neutron-induced reactions at higher energies. Generally neutron data at these energies are scarce, but charged-particle data may exist. For example, in the $^{45}\text{Sc}(p,n)$ reaction listed above, experimental data exist up to 50 MeV.⁹

The calculations were made using unadjusted "global" values for optical and preequilibrium model parameters. Comparisons with experimental data⁹⁻¹² for ^{45}Sc , ^{89}Y , ^{169}Tm , and ^{197}Au are shown in Fig. 3. The agreement is generally

good, and extends to higher energies as shown in the comparison with the ⁴⁵Sc(p,n) cross section at 25 MeV.

Thus, as has generally been the case for calculations of (n,p), (n,2n), and (n,3n) reactions, the results appear to be accurate to approximately 20% without special adjustment of model parameters.

D. Optical Model and Coupled-Channel Analysis (D. G. Madland and P. G. Young)

Work is continuing on the generation of global neutron-nucleus optical potentials in 1-p shell nuclei. At present, studies are in progress on compound elastic contributions (for $E_n < 15$ MeV in $n + {}^{12}\text{C}$ data) using the code RAROMP.¹³ At the same time the global optical model search code BOMB¹⁴ is being tested and optimized for use in eventual production runs.

The modification of the coupled-channel code JUKARL¹⁵ to output the S-matrix and compute transmission coefficients is completed. Transmission coefficients are calculated for each set of entrance-channel quantum numbers (J,π), where J can include the coupling of up to six different states with j_n of the incoming neutron. Transmission coefficients generated by RAROMP and JUKARL (with $0^+ - 2^+$ coupling) are being compared for $n + {}^{12}\text{C}$ and $n + {}^{238}\text{U}$ scattering.

E. $n + {}^{237}\text{Np}$ Evaluation (L. Stewart and P. G. Young)

The ENDF/B-IV evaluation for ${}^{237}\text{Np}$ has been modified to include new values of total $\bar{\nu}_t$ measured at Los Alamos.¹⁶ The revised $\bar{\nu}_t$ expression is compared in Fig. 4 to the ENDF/B-IV evaluation and to the new experimental data.

In addition to the $\bar{\nu}_t$ revision, the inelastic cross sections were modified between 750 keV and 3 MeV, which resulted in a somewhat harder (n,n') spectrum. The purpose of this revision was to smooth out an abrupt, discontinuous transition from a level-plus-continuum representation to a pure continuum which occurs at 1 MeV in the Version IV data.

F. Neutron Kermas from ENDF/B Data (P. G. Young and R. E. MacFarlane)

In response to a request from TD Division, we have made a preliminary study of the accuracy of neutron kermas calculated from the ENDF/B-IV evaluated data library for ${}^7\text{Li}$, ${}^{10}\text{B}$, ${}^{14}\text{N}$, ${}^{16}\text{O}$, ${}^{27}\text{Al}$, Cr, Fe, Ni, ${}^{182}\text{W}$, ${}^{183}\text{W}$, ${}^{184}\text{W}$, ${}^{186}\text{W}$, and Pb, and from the LASL ENDF/B sub-library evaluations for ${}^6\text{Li}$ and ${}^{12}\text{C}$.

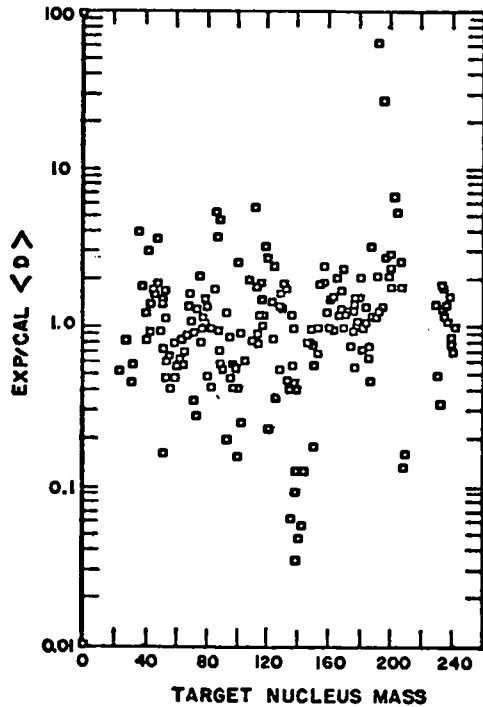


Fig. 1.

Ratio of experimental to calculated values of observed level spacing $\langle D \rangle$ obtained using parameters of Cook et al.⁷

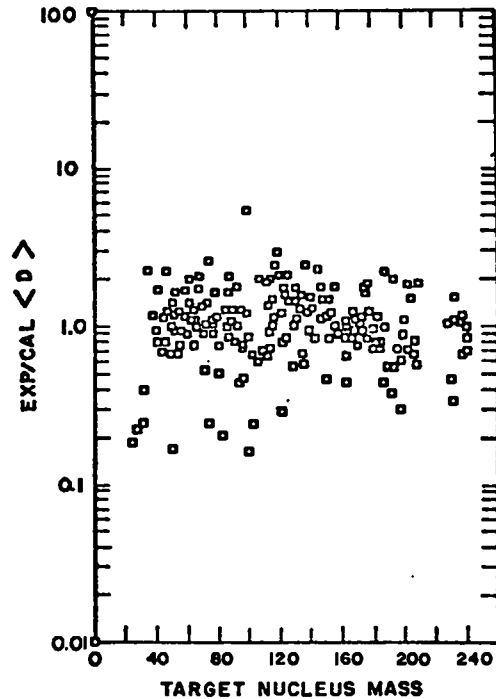


Fig. 2.

Ratio of experimental to calculated values of $\langle D \rangle$ using methods described in text.

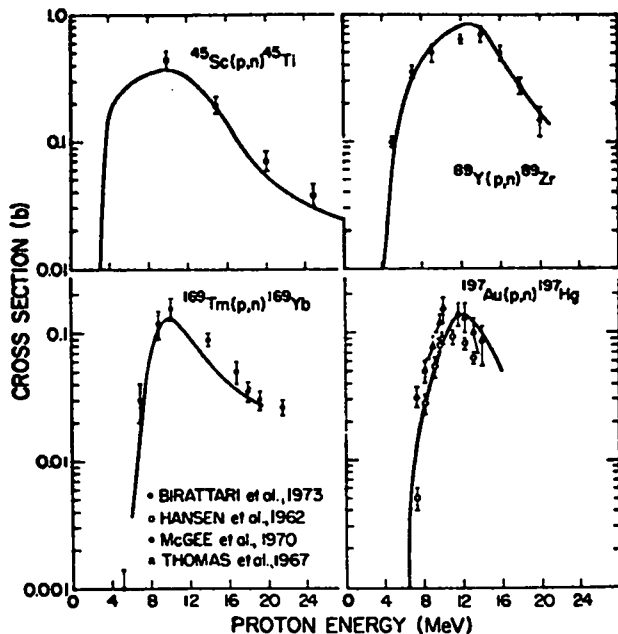


Fig. 3.

Comparison of experimental and GNASH calculated (p,n) cross sections.

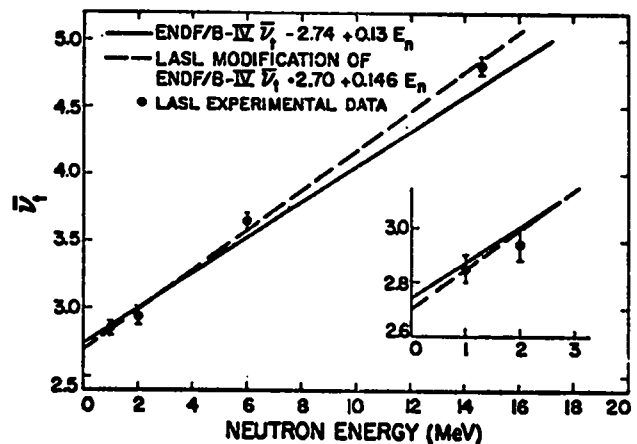


Fig. 4.

Comparison of $\bar{\nu}_1$ total for evaluated libraries with recent experimental data.

The neutron keramas were calculated from the ENDF data using the HEATR module¹⁷ of the NJOY processing code. Because detailed charged-particle data are not included in the ENDF files, neutron keramas are computed in NJOY by subtracting the emitted neutron and gamma-ray energy from the total available energy. This technique requires that total energy conservation be accurately maintained in the files, and it is a sensitive test of the internal consistency of the neutron and gamma-ray files.

To test the neutron keramas deduced from ENDF/B-IV, comparison values were calculated using more direct algorithms that require information on emitted charged-particle spectra but that do not require strict conservation of total energy. The ENDF/B-IV data for isotopes lighter than ²⁷Al are sufficiently detailed that the "direct" calculations could be performed without additional information, but it was necessary to carry out nuclear model calculations to supplement ENDF data for the heavier materials. Model calculations were performed at 8 and 14 MeV with the GNASH statistical-preequilibrium theory code¹⁸ using global model parameters. The nuclei calculated were ²⁷Al, ⁵²Cr, ⁵⁴Fe, ⁵⁶Fe, ⁵⁸Ni, ⁶⁰Ni, ¹⁸²W, ¹⁸³W, ¹⁸⁴W, ¹⁸⁶W, ²⁰⁶Pb, ²⁰⁷Pb, and ²⁰⁸Pb. Preliminary results of this study may be summarized as follows:

1. For the light isotopes up to and including ¹⁶O, the NJOY/HEATR results are in almost perfect agreement with the direct calculations. Some adjustment of the (n,γ) Q-values, however, would improve local heating values at the very lowest incident neutron energies.
2. For all heavier nuclei, serious differences in neutron keramas occur at one or more energies due primarily to inconsistencies between the ENDF/B neutron and gamma-ray data, that is, total energy conservation is not maintained in the evaluations.
3. In some cases, charged-particle reactions such as (n,np) are thought to be seriously in error at neutron energies near 14 MeV.
4. For the element evaluations, an additional problem exists due to ambiguity in the Q-values ascribed to the non-elastic reactions, particularly radiative capture.

We plan to continue this study in order to more thoroughly delineate the problems in the neutron and gamma-ray evaluated data files.

G. Evaluated Time-Dependent Electron and Photon Spectra Following A Fission Burst (D. G. Foster, Jr; M. G. Stamatelatos; and T. R. England)

We have resumed work on the time dependence of the photon spectrum emitted following fission of ²³⁹Pu by a thermal-neutron burst, using the same technique

previously reported¹⁹ for ^{235}U . Stored output from CINDER for a 10-ms burst was processed by FPSPEC to generate the time-dependent photon spectrum from 1 to 10^{11} s after fission, using the spectrum summed over 180 dominant nuclides normalized to the energy-emission rate for all 825 fission-product nuclides in the CINDER data base. Spectra for the 180 nuclides were generated beforehand from ENDF/B data. At 50 s after fission, the 180 representative nuclides account for only 49% of the total emission, so joining the CINDER results to data for earlier times may be less accurate than was the case for ^{235}U . Two codes were used earlier to describe the early and late emission. These have been combined into a single code FISPRO, which uses a cubic spline in each of 150 energy bins between 30 and 100 s after fission to smooth the transition. For an applied problem in R Division, FISPHO has been used to generate the equilibrium photon spectrum of a reactor fueled by ^{235}U operated at constant power for 6.3 yr.

In preparation for anticipated work for the Air Force Weapons Laboratory, we have begun streamlining the procedure for generating both beta and gamma spectra for fission induced by more energetic neutrons. By converting the stored spectral and intensity data to binary files, sorting them into the same order of nuclides, and storing the spectra in Large Core Memory of a CDC 7600 during processing, we have reduced the mass-storage requirements by a factor of 3 and the processing by FPSPEC by a factor of about 10. We have also added the ability to analyze more than one time-step per run.

II. NUCLEAR CROSS-SECTION PROCESSING

A. NJOY Development (R. E. MacFarlane, R. M. Boicourt, R. J. Barrett, and D. W. Muir)

NJOY work this quarter has stressed validation in preparation for the production of several new cross-section libraries. Work on the thermal reactor modules (THERMR, POWR) is discussed in Sec. II B; tests on the HEATR energy and photon interaction capabilities of GROUPE and GAMINR are discussed in Sec. II C. This intensive validation effort has uncovered many bugs -- most of them with minor effects. Both analysis and comparison with older codes have been used, and the current version of NJOY seems to work well. The next step in this validation program is to use the new libraries now being produced to make integral tests on the NJOY cross sections.

B. Thermal Power Reactor Cross Sections (R. E. MacFarlane, R. M. Boicourt, R. J. LaBauve, and D. George)

The codes for producing libraries for the EPRI-CELL code²⁰ have been completed and tested. A number of changes to the THERMR, POWR, and GROUPT modules of NJOY were required, but the data now being generated are reasonably consistent with the existing libraries. The most obvious difference is in the thermal scattering matrices. Since the NJOY matrices are group-averaged, they show appreciably more up-scatter than the energy-to-energy matrices in the existing library. The effects of these differences on integral parameters are now being explored.

The thermal calculation in EPRI-CELL has been modified to use interpolation to obtain temperatures not available in the library. This makes it possible to analyze temperature dependence in reactors with fewer data in the library. In addition, explicit resonance parameters are no longer needed for major resonance absorbers like ²⁴⁰Pu. Accurate point-kernel Doppler broadening is used, and multi-level effects are automatically included.

C. NJOY Photon Processing Validation (R. J. Barrett and R. E. MacFarlane)

In order to test the quality of photon-production and photon-interaction cross sections from NJOY, comparisons have been made with existing codes and with hand calculations.

1. Photon Production. Group constants and transfer matrices generated by NJOY under a variety of conditions were compared with hand calculations. Both constant and 1/E weighted data were tested. Continuous secondary energy distributions were checked, as well as discrete photon data (including transition probability arrays). The adjustment of photon energy due to incident neutron energy according to the equation

$$E' = E + \frac{AWR}{AWR + 1} E_n ,$$

was also checked, especially for photons in the vicinity of group boundaries. A number of interpolation schemes were also spot-checked. Results of these tests were very encouraging, although some corrections to NJOY were required.

2. Photon Interaction. The existing GAMLEG²¹ code produces photon-interaction group constants and transfer matrices using the Klein-Nishina formalism, but not including the form factor²² information from ENDF/B-IV. NJOY on

the other hand, does process these form factors. To check NJOY against GAMLEG, NJOY was modified in a minor way so as to calculate secondary energy distributions according to the exact Klein-Nishina formalism (ignoring form factors). In this approximation, NJOY output fell into remarkably good agreement with GAMLEG and with hand calculations. Furthermore, the cross sections calculated by NJOY using the form factors differed only slightly from the exact Klein-Nishina formalism, and only in forward scattering (in-group). The magnitude of these differences was verified by hand calculation.

As a result of this study, a number of errors in NJOY have been eliminated.

D. CCCC Interface Files (R. J. Barrett and R. E. MacFarlane)

Development of the MATXS cross-section interface file has continued during this quarter. One important specification of MATXS is the ability to represent all partial reactions defined in the ENDF/B format. This is straight forward for many reactions; for example, MT107 translates as "NA." However, inelastic scattering reactions can leave a residual nucleus which decays by particle emission. Such reactions are represented by "LR" flags in ENDF.²³ For example, MT57/LR22 is $(n,n')\alpha$. GROUPE and CCCCR in NJOY have been modified to process these LR flags. The MATXS file will now contain reaction names such as "N57A," "N62PP," or even "N51NNN." Codes which read MATXS can sum all reaction types containing "A" to get helium production. Sensitivity codes can make use of any partial reaction required.

E. NJOY Plotting Module (R. M. Boicourt and R. E. MacFarlane)

When dealing with large amounts of data, graphical presentation is a necessity. The LASL processing code NJOY has been routinely producing graphs of multigroup cross sections and matrices for some time. These graphs have proved very useful in checking the data as well as for giving the data user a handy reference. This plotting capability is now being extended for the use of the data evaluation in the new PLOTR module of NJOY. PLOTR allows the user to request data by ENDF/B MAT, MF, and MT number: files 3, 9, 10, 12, and 13 are 2-dimensional plots, and files 4, 5, 6, 15, and 16 are isometric. Experimental data points can be overlaid on the two-dimensional points using the Livermore data files²⁴ or the Los Alamos data files.²⁵ Figures 5 and 6 are examples of the types of plots produced. The code operates on either Version IV or Version V

NEUTRON CROSS SECTIONS

6-C-MAT
 MAT1274, MF3, MT2
 1 REF. 69057903 2 REF. 69300400
 2 REF. 69056000 3 REF. 63165600
 4 REF. 69370000

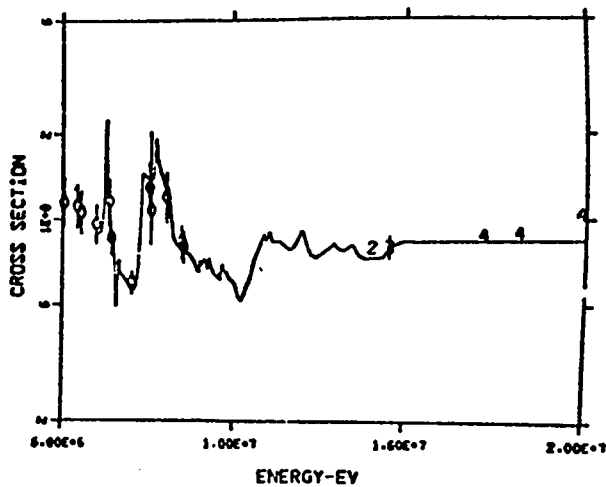


Fig. 5.

Plot comparing the elastic cross section of $^{12}_6\text{C}$ from ENDF/B-IV (MAT 1274) to experimental points from the Livermore data library.²⁴

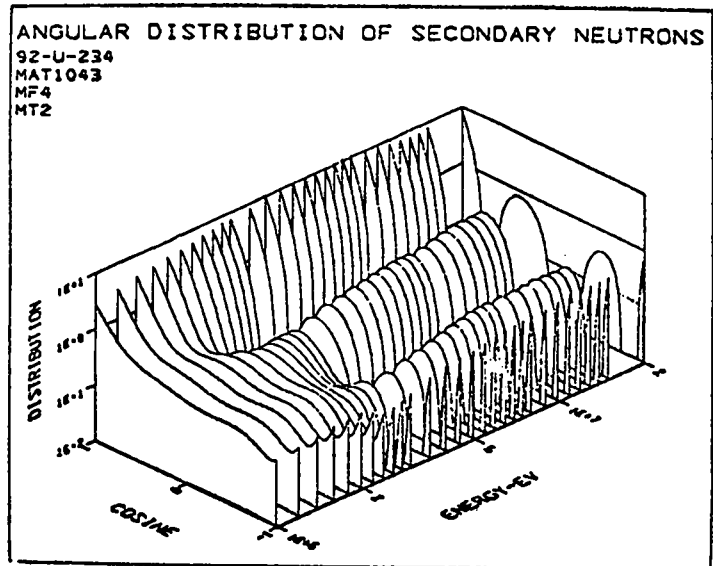


Fig. 6.

Isomeric plot of an angular distribution from ENDF/B-IV illustrating the PLOTR capability for plotting "families" of curves.

ENDF tapes and is compatible with film or CRT terminal output. The plotting utilities were designed to be partially machine-independent and are being developed into a general plotting package to be used throughout the NJOY code.

F. Photon Data for Uranium Survey (R. J. Barrett)

Los Alamos Scientific Laboratory (LASL) group R-1 is presently involved in a program to evaluate the potential for identifying natural uranium deposits by detecting characteristic gamma rays. The proposed methodology is to use the ONETRAN transport code to predict the gamma energy spectrum (in 240 groups) produced by transporting discrete photons through sandstone. To meet the data needs for this calculation, several temporary changes have been implemented in NJOY in order to produce 240-group photon interaction cross sections in the CCC-standard ISOTXS format for input to ONETRAN.

An 8-material, 14-group library was generated and successfully run through ONETRAN. Results of that run showed good agreement with a Monte Carlo calculation using MCN. The results showed a strongly suppressed photon flux in the lowest energy groups (100 eV to 200 keV). This raised a question as to

whether it was a good approximation to neglect the production of photons by Bremsstrahlung of photoelectrons. To test the approximation, the coupled gamma-electron Monte Carlo code MCGE was run by W. L. Thompson of LASL Group TD-6. Results confirmed that we were justified in neglecting Bremsstrahlung.

Subsequently, a 1-material, 240-group library has been produced for testing in ONETRAN.

G. Elastic Scattering Matrix For LDX (R. B. Kidman)

The group-to-group transfer of elastically scattered neutrons is handled in LDX²⁶ with a single elastic removal cross section for each group. This treatment appears to be satisfactory when dealing with heavy isotopes and broad groups, for then elastic transfer only occurs to the next lower group.

However, this treatment breaks down in a situation where the flux shape is significantly influenced by isotopes that elastically scatter neutrons over many downgroups. This can happen when one has narrow groups and/or light isotopes. Consider, for example, calculating the multiplication eigenvalue for a simple sphere of mixed oxide fuel ($\text{PuO}_2 + \text{UO}_2$) containing 5 weight per cent water. If one uses LIB-IV²⁷ cross sections in the original LDX, he will find that the iteration between elastic removal cross sections and flux will not converge but rather will do something like "flip-flop." This occurs because the flux determining elastic scattering cross section (mostly hydrogen) is not spread across several downscattering groups as it needs to be for this special case.

In order to determine the effect of including several elastic downscattering terms, the computer code CINX²⁸ has been modified to pass on the elastic transfer matrix from LIB-IV to LDX, and LDX has been modified to accommodate the matrix. The modified version of LDX does not iterate between the flux and elastic downscattering terms. This is the best way for now, since the present LDX iteration scheme generates downscatter cross sections that are further from reality than the original terms from LIB-IV,

Results of using the modified LDX on the mixed oxide water problem are shown in Table I. The original LDX uses 10 inelastic and 1 elastic downscattering terms. In the second case, the modified LDX uses 10 inelastic and 10 elastic downscattering terms. In the third case, the modified LDX uses 49 inelastic and 49 elastic downscattering terms. As a reminder, none of these cases iterated between flux and downscatter terms. All materials in the composition (not just hydrogen) were given the expanded downscatter treatment.

TABLE I

ELASTIC SCATTERING MATRIX EFFECTS

<u>Case</u>	<u>K_{eff}</u>
1 Original 1DX	0.8429
2 1DX with 10 elastic downscatter terms	1.0492
3 1DX with 49 elastic downscatter terms	1.0596

Since the results are rather striking, a permanent 1DX change may be in order. A number of questions are being investigated in preparation for such a change:

- . Is there a more efficient format for the increased 1DX input?
- . Would it be necessary to develop a flux iteration scheme (spectral correction) for every term of the elastic and inelastic scattering matrices?
- . Could the elastic and inelastic scattering matrices be combined prior to use in 1DX?
- . Would it be necessary to provide a table of self-shielding factors for every term of the elastic and inelastic scattering matrices?
- . Will the improved calculations justify an associated increase in computer running time plus a decrease in problem size capability?

H. ENDF/B-IV Update (R. B. Kidman)

Another set of corrections for the ENDF/B data were received this quarter. As before, the changes have been incorporated into the LASL data storage system, PHOTOSTORE. The affected PHOTOSTORE files (T401, T403, T404, T407, T408, T410, and T412) are available to all LASL personnel.

III. MAGNETIC FUSION ENERGY -- EPR COVARIANCE DATA LIBRARY (D. W. Muir)

In support of the LASL program to assess the nuclear data requirements for the design of a fusion Experimental Power Reactor (EPR), we have assembled a library of multigroup cross-section covariance data (uncertainties). Materials now contained in the covariance library are carbon, oxygen, aluminum, and iron. Uncertainty data for carbon and oxygen were taken from ENDF/B-IV (MAT=1274 and

1276, respectively); aluminum from a LASL evaluation,²⁹ in ENDF/B-IV format; and iron from an Oak Ridge National Laboratory (ORNL) evaluation³⁰ in ENDF/B-IV format.

The ORNL iron evaluation, which was prepared specifically for fast-reactor studies, contains no error information on the high-threshold reactions (n,2n) and (n,n'cont.), which are very important in fusion applications. (The cross sections at 14 MeV are 0.43 and 0.63 b, respectively.) We have added subsections to the error file for iron (MF=33) to describe these 2 reactions. These new data also make possible a more reasonable estimate of the uncertainty in the elastic scattering cross section. The latter cross section is derived by subtracting the total nonelastic cross section from the total at all energies above 1 keV.

The 4 error evaluations described above have been processed into the LASL 30-energy group neutron multigroup cross-section structure, using the ERRORR³¹ module of NJOY. ERRORR has the unique advantage of directly processing energy-dependent "derivation formulas," which are important features of both the aluminum and iron evaluations. The GROUPT module of NJOY has been used to prepare transfer matrices for each individual scattering reaction for these materials, as is required for input to sensitivity calculations.^{32,33}

All of the above data have been stored in a standard covariance library format. This format consists of three separate sections containing (a) multigroup reaction cross sections, (b) relative covariance matrices for all reactions and all cross-reaction pairs, and (c) scattering-reaction transfer matrices. Each data block within a section is preceded by a formatted identification record containing the ENDF/B reaction (MT) numbers for the reaction or reaction-pair, as well as the Legendre order of the transfer matrices.

IV. FISSION-PRODUCT, ACTINIDE, AND DECAY DATA

A. Fission-Yield Theory (D. G. Madland, R. E. Pepping [University of Wisconsin], C. W. Maynard [University of Wisconsin], T. R. England, and P. G. Young)

In order to achieve a more realistic scission configuration, fragments are allowed to assume some degree of octupole deformation in addition to the P_2 and P_4 deformations previously allowed. The fragment mass dependence with respect to P_2 and P_4 deformation is explicitly calculated by Seeger and Howard,³⁴ and P_3 dependence is assumed to be given from liquid-drop considerations.

Within the context of the statistical model, the object is to find the dependence of the excitation function with respect to the deformation parameters for a given mass and charge split. The product of the maximum value and width of the excitation function is expected to display known systematics of the yield distribution.

As the number of possible combinations of deformation parameters is large ($\sim 10^6$), a simple scheme is being sought for determining the optimum configuration.

During this quarter, the required data file became larger than the user's allotment on the available machines. Files were consequently reformatted and placed on tape. The current file contains a listing of information on fragment pairs: included for each fragment are the calculated ground-state shape and binding energy, as well as individual terms contributing through the mass formula,³⁴ such as the pairing and single-particle correction terms. Also, the same quantities are calculated on a grid of 20 values of ϵ and 5 values of ϵ_4 , in order to study the excitation function for highly deformed shapes.

B. ENDF/B Phenomenological Yield Model Improvements

1. Distribution of Independent Fission-Product Yields to Isomeric States (D. G. Madland and T. R. England). This work has been completed and reported in Refs. 35 and 36.

2. Pairing Effects on the Distribution of Fission-Product Yields (D. G. Madland and T. R. England). This work has been completed and reported in Refs. 37 and 38.

3. Z_p Values for Neutron-Induced Fission (D. G. Madland and R. E. Pepping [University of Wisconsin]). The mass formula of Seeger and Howard³⁴ has been used to calculate 750 Q values for fragments produced in binary fission. For each isobaric chain of the fragment yield, the most probable Q value Q_p has been assumed related to the most probable charge Z_p by

$$Q - Q_p = - (Z - Z_p)^2 / 2\sigma^2 \quad . \quad (1)$$

For a given mass chain (roughly 15 masses), Q_p , Z_p , and σ are adjusted to give the best fit to Eq. (1). The most probable charge for the complementary mass chain is then given by $(Z_c - Z_p)$ where Z_c is the charge of the fissioning compound system. Calculations have been performed for the thermal-neutron-induced

fission of ^{235}U and ^{241}Am . The fitting procedure has been applied for mass chains 70 to 170, for Z-even, Z-odd, as well as all Z, in a given mass chain. The results are now being studied. At this time it appears that the width σ is a function of A and that its average value is somewhat less than that used in the ENDF/B-IV Fission Product Files³⁹ (0.56). In addition, comparisons of our Z_p values to those of ENDF/B-IV show differences as large as 0.6 charge units. It should be noted that our Z_p values differ from the desired Z_p values in two ways: (1) we calculate Z_p for fission fragments, not fission products; and (2) the calculated fragment Z_p values are valid only for the fragment in its ground state.

C. Fission-Product Data for Thermal Reactors (T. R. England, W. B. Wilson, M. G. Stamatelatos, and N. L. Whittemore)

A four-group fission-product absorption-chain library using ENDF/B-IV decay data and cross sections processed with a typical light-water reactor spectrum has been completed. The library is formatted for use in a modified version of the original CINDER code. This project, funded by the Electric Power Research Institute (EPRI), includes an 84-chain library appropriate for the modified code and a 12-chain library (which includes 1 pseudo chain) appropriate for spatial depletion codes. Two reports describing the project have been completed; these are to be issued by EPRI. The project included survey calculations of absorption buildup and a comparison with a long-term irradiation experiment.

D. Fission-Product Absorption Cross Sections for PWR Applications (W. B. Wilson)

A library of fission-product cross sections has been produced in each of two 2-group structures for the Power Generation Group of Babcock and Wilcox (B&W). ENDF/B-IV fission-product cross sections, previously processed⁴⁰ into the Power Reactor Studies (PRS) 154 Group Structure⁴¹ with the PRS Flux Weighting Function⁴² by the NJOY code,⁴³ were collapsed by the TOAFEW⁴⁴ collapsing code into the 2-group structures defined as follows:

	<u>Group Structure 1</u>	<u>Group Structure 2</u>
	10 MeV	10 MeV
group 1	1.855391363 eV	0.5032348036 eV
group 2	1.0×10^{-5} eV	1.0×10^{-5} eV

The weighting flux used in collapsing, furnished by B&W, described the Pressurized Water Reactor (PWR) flux spectrum in 71 histogram values. The 71-group flux is compared to the PRS Flux Weighting Function in Fig. 7, in which flux integrals over the energy range of the group structure are equated.

The TOAFEW code was modified to supply fission-product cross sections in a requestor's 1-, 2-, 3-, or 4-group structure. The neutron flux-weighting function may be specified in histogram form, with the flux in units of flux per unit energy, flux per unit lethargy, or as group integrated fluxes. The flux may also be specified by a set of log-log interpolation points, with the flux given in units of flux per unit energy. The PRS Flux Weighting Function and the Muir-Roussin Flux Function⁴⁵ are options of the code and may alternately be selected.

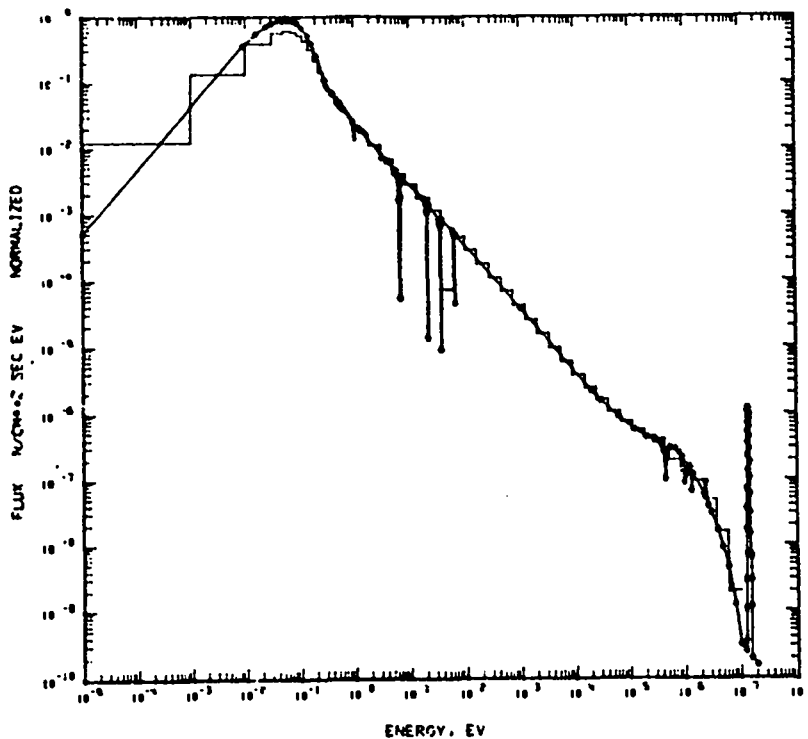


Fig. 7. Fluxes used in processing and collapsing 1154-Group LASL fission-product data for Babcock and Wilcox.

E. Photoneutron Spectra (M. G. Stamatelatos and T. R. England)

The gamma-ray spectra above 1.67 eV and corresponding photoneutron spectra from $^9\text{Be}(\gamma, n)$ and $^2\text{H}(\gamma, n)$ reactions were calculated for a variety of fuels, irradiation histories, and cooling times. This work was completed and a report submitted for a US Nuclear Regulatory Commission (NRC) review in May 1976. The report⁴⁶ was recently published by NRC.

F. HTGR Burnup Calculations (T. R. England, M. G. Stamatelatos, R. J. LaBauve, P. Bailey [Q-6], and N. L. Whittemore)

A 2-group core-averaged burnup and reload calculation for a standard 3000 MW(t) HTGR was made using the CINDER-10 computer code. The code was modified to permit specific reload changes in actinide densities and fission products. The two-group fluxes and the more important actinide cross sections are based on a collapsing of an existing LASL nine-group ENDF/B-IV based library. The fission-product library is also based on ENDF/B-IV files. Some actinide data are based on a preliminary Version V file of ENDF/B. The calculations and output include:

1. 26 actinides (from ^{232}Th through ^{244}Cm).
2. 826 fission products.
3. 34 time increments with reloads specified at 1-y intervals. (Each depletion interval consisted of 4 successive time increments of 2100-h duration; this was followed by 1 zero-power decay period of 335 h, and 1 of 1 h at the end of which the calculated reloading was made.)
4. At the end of each time-step, the output includes
 - . densities, activities, beta and gamma energies, and barns/fission of the fission products (for the actinides, the densities and activities only are included);
 - . for the rare gases and halogens, there are separate tabulations of densities, activities (in curies), and the beta and gamma energies;
 - . these results are given by nuclide and by summary tabulations of aggregate data;
 - . density sums by charge and mass are included.

The output is stored on MT for HTGR users and for analysis of higher mass actinide buildup.

G. ANS 5.1 Decay Heat Standard (T. R. England, M. G. Stamatelatos, and N. L. Whittemore)

Several calculations have been made for use in determining the new ANS Decay Heat Standard. Beta and gamma spectra and aggregate beta- and gamma-decay heating were calculated for the Intelcom Rad Tech (IRT) experiments; these were an extension of the data reported in the previous progress report.⁴⁷ Aggregate values for use in determining the standard and the effect of neutron capture were also calculated and supplied to the ANS 5.1 Working Group.

H. Source Terms for Spent Fuel Accident (T. R. England and N. L. Whittemore)

This project includes a variety of fission-product source terms in spent fuels, including details on gas content. Several calculations were completed for various fuels and irradiation times. This work is being done for reference use by the NRC.

I. CSEWG Fission Product Yields Subcommittee Meeting (T. R. England)

The Cross Section Evaluation Working Group (CSEWG) Fission Product Yields Subcommittee met at Los Alamos on December 7 and 8, 1976. The meeting was well attended, and several decisions were made concerning the data to be included in ENDF/B-V. A preliminary evaluation of 20 yield sets (twice the number in ENDF/B-IV) was discussed. The sets to be included in ENDF/B-V are listed in Table II. The number designation in Table II indicates the order of evaluation.

J. Actinide Chains (D. E. Wessol [EG&G Idaho, Inc.], T. R. England, W. B. Wilson, and M. G. Stamatelatos)

A set of 58 chains incorporating ~50 actinides (from ²³¹Th through ²⁵⁴Es) has been generated for use in fuel cycle, safeguards, and waste disposal studies. Few-group cross sections for most of these nuclides are currently being processed using preliminary ENDF/B-V data; the chains are being tested for completeness, and a search for a few decay parameters is in progress.

K. Decay-Heat Beta Spectra (M. G. Stamatelatos and T. R. England)

A series of calculations are under way to compare calculated fission-product beta-decay spectra and total beta-energy release per fission with results of recent decay-heat experiments performed at ORNL. These experiments have produced cumulative fission-product spectra measured at a number of

shutdown times following 1-, 10-, and 100-s irradiations of ^{235}U samples in a thermal neutron spectrum.

TABLE II
YIELD SETS TO BE INCLUDED IN ENDF/B-V^a

Fissionable Nuclide	Yield Type or Incident Neutron Energy			
	T	F	HE	SF
^{235}U	1	2	3	-
^{238}U	-	4	5	-
^{239}Pu	6	7	14	-
^{241}Pu	8	16	-	-
^{233}U	9	11	12	-
^{232}Th	-	10	18	-
^{236}U	-	13	-	-
^{240}Pu	-	15	-	-
^{242}Pu	-	17	-	-
^{237}Np	-	19	-	-
^{252}Cf	-	-	-	20

^aThe number denotes the current order of evaluation.

T denotes thermal fission

F denotes fast fission

HE denotes high-energy (~14 MeV) fission

SF denotes spontaneous fission

REFERENCES

1. A. V. Ignatyuk, G. N. Smirenkin, and A. S. Tishin, "Phenomenological Description of the Energy Dependence of the Level Density Parameters," Sov. J. Nucl. Phys. 21, 255 (1975).
2. A. V. Ignatyuk and V. S. Stavinskii, "Spin Dependence of the Density of Excited States of Nuclei," Sov. J. Nucl. Phys. 11, 674 (1970).
3. V. A. Rubchenya, "Effects of Structure of the Single-Particle Spectrum on the Level Density of Rare-Earth Nuclei," Sov. J. Nucl. Phys. 11, 571 (1970).
4. H. Baba, "A Shell-Model Nuclear Level Density," Nucl. Phys. A159, 269 (1973).
5. W. Dilg, W. Schantl, H. Vonach, and M. Uhl, "Level Density Parameters for the Back-Shifted Fermi Gas Model in the Mass Range $40 < A < 250$," Nucl. Phys. A217, 269 (1973).
6. A. Gilbert and A. G. W. Cameron, "A Composite Nuclear-Level Density Formula with Shell Corrections," Can. J. Phys. 43, 1446 (1965).
7. J. L. Cook, H. Ferguson, and A. R. deL. Musgrove, "Nuclear Level Densities in Intermediate and Heavy Nuclei," Aust. J. Phys. 20, 477 (1967).
8. L. G. Moretto, "Statistical Description of Deformation in Excited Nuclei and Disappearance of Shell Effects with Excitation Energy," Nucl. Phys. A182, 641 (1972).
9. T. McGee, G. L. Rao, G. B. Saba, and L. Yaffee, "Nuclear Interactions of ^{45}Sc and ^{68}Zn with Protons of Medium Energy," Nucl. Phys. A150, 11 (1970).
10. R. G. Thomas, Jr. and W. Bartolini, "Neutron Production in Ag, Ta, Au, Pt, and Pb by the Interaction of 7.5-14 MeV Protons," Phys. Rev. 159, 1022 (1967).
11. C. Birattari, E. Gadioli, E. Gadioli Erba, A. M. Grassi Strini, G. Strini, and G. Tagliaferri, "Pre-equilibrium Processes in (p,n) Reactions," Nucl. Phys. A201, 579 (1973).
12. L. F. Hansen, R. C. Jopson, Hans Mark, and C. D. Swift, " $\text{Ta}^{181}(p,n)\text{W}^{181}$ and $\text{Au}^{197}(p,n)\text{Hg}^{197}$ Excitation Functions Between 4 and 13 MeV," Nucl. Phys. 30, 389 (1962).
13. G. J. Pyle, "RAROMP (Regular and Reformulated Optical Model Potentials," John H. Williams Laboratory of Nuclear Physics Internal report, University of Minnesota (private communication) (1968).
14. F. D. Becchetti, Jr., University of Michigan (private communication) (1976).

15. H. Rebel and G. W. Schweimer, "Improved Version of Tamura's Code for CoupledChannel Calculations: JUPITOR Karlsruhe Version," Gesellschaft fur Kernforschung M.B.H. report KFK 133 (February 1971).
16. L. R. Veaser, Los Alamos Scientific Laboratory, private communication (1976).
17. C. I. Baxman and P. G. Young, Eds., "Applied Nuclear Data Research and Development Quarterly Progress Report," Los Alamos Scientific Laboratory report LA-6266-PR (1976), p. 8.
18. E. D. Arthur and P. G. Young, "A New Statistical Preequilibrium Nuclear Model Code," Trans. Am. Nucl. Soc. 23, 500 (1976).
19. C. I. Baxman and P. G. Youngs, Eds., "Applied Nuclear Data Research and Development Quarterly Progress Report," Los Alamos Scientific Laboratory report LA-6560-PR (1976), p. 6.
20. EPRI-CELL is a proprietary code developed by Nuclear Associates International, Rockville, Md., for the Electric Power Research Institute. Information can be obtained from the owners.
21. K. D. Lathrop, "GAMLEG - A FORTRAN Code to Produce Multigroup Cross Sections for Photon Transport Calculations," Los Alamos Scientific Laboratory report LA-3267 (April 1965).
22. J. H. Hubbell, W. J. Veigele, E. A. Briggs, R. T. Brown, D. T. Cromer, and R. J. Howerton, "Atomic Form Factors, Incoherent Scattering Functions and Photon Scattering Cross Sections," J. Phys. Chem. Ref. Data 4, 471 (1975).
23. D. Garber, C. Dunford, and S. Pearlstein, "Data Formats and Procedures for the Evaluated Nuclear Data File, ENDF," Brookhaven National Laboratory report BNL-NCS-50496 (ENDF 102) (1975), p. 3.9.
24. M. H. MacGregor, D. E. Cullen, R. J. Howerton, and S. T. Perkins, "An Integrated System for Production of Neutronics and Photonics Computational Constants," Lawrence Livermore Laboratory report UCRL-50400 (July 1976).
25. P. G. Young, Los Alamos Scientific Laboratory, private communication (1976).
26. R. W. Hardie and W. W. Little, "LDX, A One-Dimensional Diffusion Code for Generating Effective Nuclear Cross Sections," Battelle Northwest Laboratory report BNWL-954 (March 1969).
27. R. B. Kidman and R. E. MacFarlane, "LIB-IV, A Library of Group Constants for Nuclear Reactor Calculations," Los Alamos Scientific Laboratory report LA-6260-MS (1976).
28. R. B. Kidman and R. E. MacFarlane, "CINX: Collapsed Interpretation of Nuclear X-Sections," Los Alamos Scientific Laboratory report LA-6287-MS (1976).

29. D. G. Foster, Jr., Los Alamos Scientific Laboratory, private communication (1976).
30. C. Y. Fu, Oak Ridge National Laboratory, private communication (1976).
31. C. I. Baxman and P. G. Young, "Applied Nuclear Data Research and Development Quarterly Progress Report," Los Alamos Scientific Laboratory report LA-6266-PR (March 1976) p. 5.
32. S. A. W. Gerstl, Los Alamos Scientific Laboratory, private communication (1976).
33. D. E. Bartine, E. M. Oblow, and F. R. Mynatt, "Radiation-Transport Cross-Section Sensitivity Analysis - A General Approach Illustrated for A Thermo-nuclear Source in Air," Nucl. Sci. Eng. 55, 147 (1974).
34. P. A. Seeger and W. M. Howard, "Table of Calculated Nuclear Properties," Los Alamos Scientific Laboratory report LA-5750 (October 1974).
35. D. G. Madland and T. R. England, "Distribution of Independent Fission-Product Yields to Isomeric States," Los Alamos Scientific Laboratory report LA-6595-MS (ENDF 241) (November 1976).
36. D. G. Madland and T. R. England, "Distribution of Independent Fission-Product Yields to Isomeric States," Trans. Am. Nucl. Soc. 24, 461 (1976).
37. D. G. Madland and T. R. England, "The Influence of Pairing on the Distribution of Independent Yield Strengths in Neutron-Induced Fission," Los Alamos Scientific Laboratory report LA-6430-MS (ENDF 240) (July 1976).
38. D. G. Madland and T. R. England, "Pairing Effects on the Distribution of Fission-Product Yields," Trans. Am. Nucl. Soc. 24, 462 (1976).
39. M. E. Meek and B. F. Rider, "Compilation of Fission Product Yields Vallecitos Nuclear Center 1974," General Electric report NEDO-12154-1, (January 1974).
40. C. I. Baxman, G. M. Hale, and P. G. Young, Eds., "Applied Nuclear Data Research and Development Quarterly Progress Report," Los Alamos Scientific Laboratory report LA-6472-PR (1976) p. 60.
41. R. J. LaBauve and W. B. Wilson, "Proposal to Extend CSEWG Neutron and Photon Multigroup Structures for Wider Applications," Los Alamos Scientific Laboratory report LA-6240-P (1976).
42. C. I. Baxman, G. M. Hale, and P. G. Young, Eds., "Applied Nuclear Data Research and Development Quarterly Progress Report," Los Alamos Scientific Laboratory report LA-6472-PR (1976) p. 47.
43. R. E. MacFarlane and R. M. Boicourt, "NJOY: A Neutron and Photon Cross-Section Processing System," Trans. Am. Nucl. Soc. 22, 720 (1975).
44. W. B. Wilson, Los Alamos Scientific Laboratory, private communication (1976).

45. R. Roussin, Oak Ridge National Laboratory, private communication (1976).
46. M. G. Stamatelatos and T. R. England, "Fission-Product Gamma-Ray and Photoneutron Spectra and Energy-Integrated Sources," Los Alamos Scientific Laboratory report NUREG-0155 (LA-NUREG-6345-MS) (December 1976).
47. C. I. Baxman and P. G. Young, Eds., "Applied Nuclear Data Research and Development Quarterly Progress Report," Los Alamos Scientific Laboratory report LA-6723-PR (1977).